

cloud, and the possible high altitude or inhomogeneity of an ammonia cloud are important and indicative of the extreme variability of the jovian atmosphere.

REFERENCES AND NOTES

1. B. Ragent *et al.*, *Space Sci. Rev.* **60**, 179 (1992).
2. T. V. Johnson *et al.*, *ibid.*, p. 3.
3. W. J. O'Neill and R. T. Mitchell, in *Proceedings of the AIAA 21st Aerospace Sciences Meeting*, Reno, NV, 10 to 13 January 1983 (American Institute of Aeronautics and Astronautics, New York, 1983), pp. 1-10; J. J. Givens *et al.*, *ibid.*, pp. 1-18.
4. A. Seiff *et al.*, *Science* **272**, 844 (1996). All atmospheric pressure, temperature, and altitude information were obtained from this reference.
5. During descent in the jovian atmosphere, the range of temperatures experienced by the instrument mounted in the probe extended from about -50°C to over 100°C . Rates of temperature excursions were as large as 6°C per minute. This temperature behavior has complicated the interpretation of the data, but the instrument functioned properly down to at least the 10-bar level.
6. L. A. Sromovsky *et al.*, *Science* **272**, 851 (1996).
7. S. J. Weidenschilling and J. W. Lewis, *Icarus* **61**, 311 (1973); S. K. Atreya and P. N. Romani, in *Photochemistry and Clouds of Jupiter, Saturn and Uranus in Recent Advances in Planetary Meteorology*, G. Hunt, Ed. (Cambridge Univ. Press, Cambridge, 1985), pp. 17-68.
8. H. B. Niemann *et al.*, *Science* **272**, 846 (1996).
9. Using techniques similar to those used by M. Ya Marov *et al.* [*Icarus* **44**, 608 (1980)], we have derived scattering cross sections from the raw data of Fig. 1 for the cloud at 1.4 bars. We assumed that the particle density immediately below the cloud base is zero and that the signals in the cloud larger than that at the base are due to cloud particles, and we included temperature-dependent corrections for baseline offsets and channel sensitivities. Large errors due to out-of-range corrections may be present in these data. We have compared these cross sections with those calculated for conservative scattering from model particle size distributions to obtain best fit values for the model parameters. A typical set of derived cloud property values obtained at this location, by using a log normal particle size distribution and the data described above and assuming a particle mass density of 1.0, are characteristic radius, $r_m = 4.5 \mu\text{m}$; characteristic width parameter, $\sigma = 1.5$; particle number density, $N = 2.5 \times 10^6 \text{ m}^{-3}$; local particle mass loading mass density, $\rho = 9.5 \times 10^{-7} \text{ kg m}^{-3}$; scattering optical depth, $\tau \approx 2.6$; columnar particle loading, $N_0 = 1.4 \times 10^{10} \text{ m}^{-2}$; and columnar mass loading, $W_0 = 5.3 \times 10^{-3} \text{ kg m}^{-2}$. We emphasize that the values quoted here, although not inconsistent with values derived from earlier analyses of Voyager mission data (11), may be subject to major revision and should only be taken as illustrative of the analytical process results until full consideration of corrections for the instrumental temperature profiles, optical surface coatings, or other effects not yet fully analyzed have been completed.
10. Observations of thermal emission from the entry site with Earth-based telescopes [G. Orton *et al.*, *Science* **272**, 839 (1996)] characterized the probe entry site as being within and near the edge of a $5\text{-}\mu\text{m}$ "hot spot" (an area observable at a wavelength of $5 \mu\text{m}$), a region considerably brighter than its surroundings, indicating that particles or absorbing gases are reduced in concentration in this region.
11. B. E. Carlson *et al.*, *J. Geophys. Res.* **98**, 5251 (1993).
12. We acknowledge the extensive contributions of our deceased co-investigator, colleague, and friend, James B. Pollack. We are grateful for the dedicated efforts of many of the members of the staff of the Martin-Marietta Aerospace Division, Denver, CO, and of the Galileo Probe Project Office and the Electronic Instrument Development Branch of NASA Ames Research Center for the design, construction, testing, and calibration of the Galileo probe neph-

elometers and for the successful mission activities. We also wish to thank the following people at NASA Ames Research Center: M. Smith, C. Soback, P. Melia, M. Izadi, B. Chin, and E. Tischler of the Galileo Probe Project Office, L. Colin, retired chief of the Space Sciences Division, and G. Deboo and W. Gunter, of the Electronic Instrument Development

Branch. Thanks also to T. Knight, J. Martin, J. Waring, and C. Carlston of the Martin-Marietta Aerospace Division. Supported under NASA cooperative research agreement NCC 2-466 and NASA contract NAS 2-10015.

4 March 1996; accepted 17 April 1996

High-Energy Charged Particles in the Innermost Jovian Magnetosphere

H. M. Fischer, E. Pehlke, G. Wibberenz, L. J. Lanzerotti, J. D. Mihalov

The energetic particles investigation carried by the Galileo probe measured the energy and angular distributions of the high-energy particles from near the orbit of Io to probe entry into the jovian atmosphere. Jupiter's inner radiation region had extremely large fluxes of energetic electrons and protons; intensities peaked at $\sim 2.2R_J$ (where R_J is the radius of Jupiter). Absorption of the measured particles was found near the outer edge of the bright dust ring. The instrument measured intense fluxes of high-energy helium ions (~ 62 megaelectron volts per nucleon) that peaked at $\sim 1.5R_J$ inside the bright dust ring. The abundances of all particle species decreased sharply at $\sim 1.35R_J$; this decrease defines the innermost edge of the equatorial jovian radiation.

More than four decades ago, Burke and Franklin discovered that Jupiter emitted radio waves (1). Much of the nonthermal, synchrotron radiation from Jupiter originates from high-energy electrons that are trapped by the magnetic field relatively close to the planet. Of the flybys of the planet by the Pioneer 10 and 11, Voyager 1 and 2, and Ulysses spacecraft, only Pioneer 11 entered into the intense radiation region at distances close enough to the planet ($1.6R_J$) to obtain measurements of particles that could be major contributors to the nonthermal radio emissions (2). The Galileo probe, carrying the energetic particle instrument (EPI) through the jovian magnetosphere (3), provided the first measurements of the innermost regions of Jupiter's radiation environment.

The EPI instrument operated during the pre-entry phase of the mission, when the probe's heat shield still protected the descent module. Thus, the measured particles had to have energies high enough to penetrate the heat shield in order to be measured by the instrument. Three data samples were acquired near the equatorial region at 5, 4, and $3R_J$, and a continuous series of measurements (12 data samples) were obtained from 2.4 to $1.25R_J$. On the basis of pre-entry trajectory information, the spatial resolution of the data is $\sim 0.1R_J$ in the innermost region before the probe entered into the atmosphere.

H. M. Fischer, E. Pehlke, G. Wibberenz, Institut für Kernphysik, Universität Kiel, D-24118 Kiel, Germany.
L. J. Lanzerotti, Bell Laboratories, Lucent Technologies, Murray Hill, NJ 07974, USA.
J. D. Mihalov, NASA Ames Research Center, Moffett Field, CA 94035, USA.

Three different energy range channels were allocated to both electrons and protons in order to provide a rough estimate of the energy spectral dependence of each species over the energy range measured (Table 1) (4). Because of the expected low statistics, counts of heavy particles were accumulated over longer time periods than for the electrons and the protons. In addition to spin-averaged measurements, angular-scattered data were obtained for electrons, protons, and alpha particles in certain energy ranges in order to determine directional anisotropies and particle pitch angle distributions. The angular data were determined with the use of (i) magnetic field measure-

Table 1. Energy sensitivity of EPI channels, showing energy ranges for particle species having traversed the probe's aft heat shield. The given values were derived for an 18° mean angle of inclination of the particles' incoming direction with respect to the telescope axis, which is accurate for an isotropic particle distribution (15). Single energy values correspond to the lower limit for the channel. Upper energy limits exceeding 1 GeV are not contained in this table. Missing entries indicate no significant response to that species in that channel.

Channel	Energy ranges (MeV nucleon ⁻¹) for particle species				
	e ⁻	p ⁺	He	C	S
E1	3.2	42	42	75	125
E2	8	62	62	110	210
E3	8	62	62	110	210
P1	66	42-131	42	75	125
P2	100	62-131	62	110	210
P3	203	62-92	62-530	110	210
He	450	-	62-136	110	210
HV	-	-	-	110-168	210

ments that were made by the probe lightning and radio emission detector (LRD) instrument (5) at $3R_J$ and from $2R_J$ to atmospheric entry and (ii) a pseudo-spin period at 5 and $4R_J$ that was within 2% of the period measured at $3R_J$.

The detector configuration was designed to limit counting rates to less than about 3 million counts per second. This limit was nearly reached in channel E1 during most of the pre-entry mission. The probe's aft heat shield—containing layers of aluminum, adhesive, Kapton, Mylar, Dacron, and phenolic nylon with a total thickness of 1.34 cm—was equivalent to 1.87 g cm^{-2} of shielding for perpendicularly incident particles. Some of the instrument calibrations were performed with heat shield material in order to appropriately characterize the detector responses.

The spin-averaged fluxes of energetic electrons (E1-P1), protons (P1), helium (He), and $Z > 2$ ions (HV, where Z is the nuclear charge) from inside the Io torus region to the upper jovian atmosphere show a general increase of fluxes to a peak inside the orbit of Amalthea (Fig. 1). The fluxes then decreased at $\sim 2R_J$ and reached intermediate values between 2 and $1.8R_J$. Finally, a small peak in the electrons and protons, and much larger relative peaks in the He and HV ions (6), were

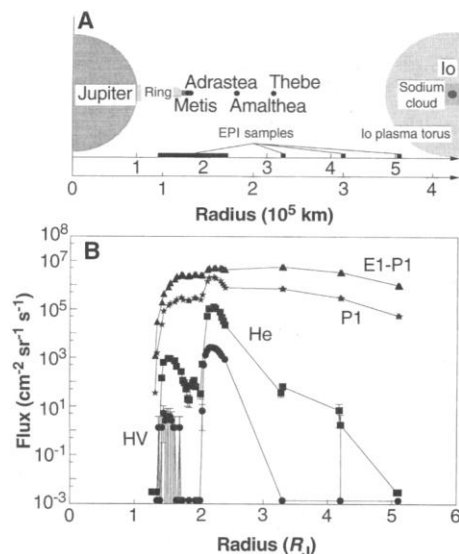


Fig. 1. High-energy particle observations in four species-energy channels (see Table 1) obtained with the EPI instrument along the Galileo probe pre-entry trajectory. **(A)** The distribution of the EPI equally spaced data samples ($\sim 1R_J$) acquired between 5 and $3R_J$ and the subsequent interval of continuous measurements from 2.4 to $1.25R_J$ are shown related to the location of the orbit of the jovian moon Io and its plasma torus; the orbits of the moons Thebe, Amalthea, Metis, and Adrastea; and the position of the dust ring. **(B)** The selected channels show the particle fluxes for energetic electrons (E1-P1), protons (P1), helium (He), and heavier particles (HV). The symbols below 10^{-2} indicate data points with zero count rate.

seen at $\sim 1.5R_J$ before the fluxes dropped sharply at $\sim 1.35R_J$. The increase in the He and HV fluxes inside the orbit of the jovian ring material was totally unexpected, although the outer peak was also observed by Pioneer 11 (7).

Since the Pioneer 11 measurements in 1974, Io and its surrounding torus have been identified not only as absorbers of trapped jovian particles, but also as sources of electrons in the energy range of kiloelectron volts (8–10). Measurements by Pioneer 11, near the perihelion distance of its jovian orbit just inside the bright ring, showed that the proton fluxes for particles between 14.8 and 21.2 MeV were higher there than just outside the ring (9, 11). The EPI measurements show that fluxes increase to the outer edge of the jovian bright ring material. Thus, the increase of particle fluxes with decreasing radial distance to the planet exhibits a somewhat shell-like structure (surrounding the planet) that depends on energy and particle species. The Pioneer 11 observations were interpreted as indicating that macroscopic objects orbiting the planet were absorbing radially inward-diffusing particles (11, 12). The EPI measurements show that such a shell-like structure is also seen in the He and HV particle rates inside the Amalthea orbit, including the new peak at $\sim 1.5R_J$ inside the ring material.

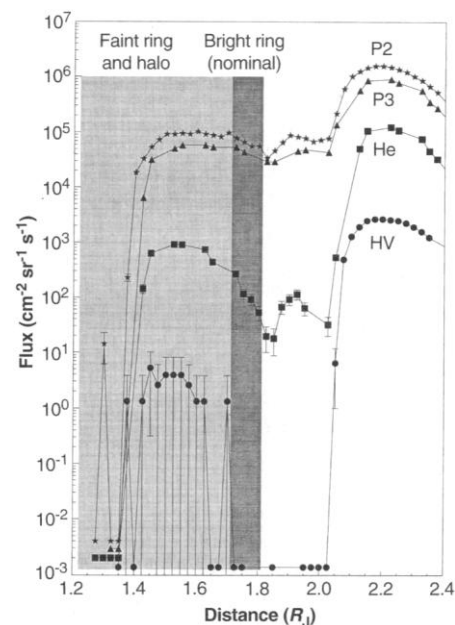


Fig. 2. Particle fluxes between 1.25 and $2.4R_J$ in the interval in which continuous data coverage was achieved with the Galileo probe EPI instrument. Presented are the observed count rates for the proton channels (P2) and (P3), as well as for the helium (He) and heavier particle (HV) channels (Table 1). The location of the jovian dust ring components is superimposed on the diagram. The symbols below 10^{-2} indicate data points with zero count rate.

Comparisons of several spin-averaged particle populations measured outside and inside the ring region, between 1.2 and $2.4R_J$ (Fig. 2) with the locations of the jovian dust ring components (13), show that the interactions of all particle species with the ring material lead to significant absorption. The major puzzle in these data is the source of the He and HV particles with intensity peaks near $1.5R_J$, which are enhanced by a factor of 10 or more over the values that they have after absorption in the vicinity of the bright ring material. Possible origins for these ions with $Z > 1$ include (i) the spallation of ring material by the energetic trapped protons and cosmic rays and (ii) cosmic ray sputtering of He from the jovian atmosphere.

The particle fluxes drop steeply inside a distance of $\sim 1.35R_J$, which is considerably above the jovian atmosphere. This indicates that the inward radial extent of the fluxes at the equator is not cut off by the equatorial atmosphere. This is similar to the situation in the Earth's magnetosphere. The cutoff in the fluxes on Jupiter is determined by the location where the dipole field line enters the atmosphere.

Evidence of the interaction of the parti-

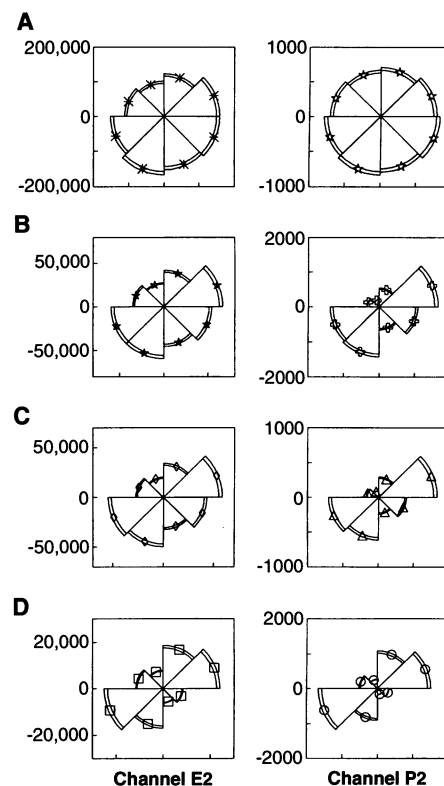


Fig. 3. Angular distributions for the E2 and P2 (Table 1) particle channels are shown for selected radial distances: $3.3R_J$ **(A)**; $1.95R_J$ **(B)**; $1.85R_J$ **(C)**; and $1.55R_J$ **(D)**. The numbers given on the axis of each distribution indicate the counts per second. The spacings between the two arcs of each sector indicate the statistical uncertainties.

cles with the atmosphere where the dipole field line enters it can be obtained from the directional variations in the particle fluxes. We determined relative directional fluxes of particles using counting rates in the E2 and P2 channels (Fig. 3) and the simultaneously measured magnetic field (5). The directional fluxes varied considerably with decreasing radial distance from the planet, becoming increasingly anisotropic closer to the planet. Thus, only particles whose velocity vectors have large angles relative to the local magnetic field can remain trapped at the closer distances.

The electron flux profile in Fig. 1B is similar to that deduced previously from Pioneer 11 measurements during its closest approach to the planet (10). The earlier Pioneer 11 profile was shown, in turn, to be consistent (for certain assumptions about the electron energy spectra and about non-radiative losses) with ground-based measurements of the jovian decimetric radio emissions (14). The data from the probe E2 electron coincidence channel are within a factor of 3 of previous Pioneer levels in the region where there is overlap. Examination of the electron spectra indicates that relatively more higher-energy as compared to lower-energy particles were measured with the probe instrument than reported from the Pioneer missions for the same energy range.

V A R E F E R E N C E S A N D N O T E S

- B. F. Burke and K. L. Franklin, *J. Geophys. Res.* **60**, 213 (1955).
- Special issue on Pioneer 10, *Science* **183** (1974); special issue on Pioneer 10, *J. Geophys. Res.* **79** (1974).
- H. M. Fischer *et al.*, *Space Sci. Rev.* **60**, 1 (1992). The EPI detector assembly consists of a two-element telescope that uses totally depleted, circular silicon surface barrier detectors. Each detector has a thickness of 0.5 mm, a radius of 1.4 mm, and a sensitive area of 6.2 mm². A 3-mm-thick (equivalent to 2.55 g cm⁻²) brass absorber is inserted between the two detectors in order to expand the energy range of particles that can be measured. The total length of the telescope (upper surface front detector to lower surface back detector) is 6 mm. The detector assembly is surrounded by tungsten shielding with a cylindrical wall thickness of 2.7 mm (equivalent to 4.86 g cm⁻²). The entire probe and its contents, estimated to be equivalent to at least 80 g cm⁻², form the rear shielding of the telescope. A number of instrument performance effects during flight—such as acceptance curves for energy channels, final geometrical factors, deadtime losses, stray coincidences, and multiparticle events, as well as the influence of the heat shield—are accounted for here only with initial estimates. The instrument temperature during the encounter was <0°C, so no thermal noise problems existed in the detectors.
- For the E1, E2, and E3 electron thresholds in Table 1, the tabulated values are obtained from range-energy relations. When the scattering of incident electrons from the aft heat shield is considered, the median energies detected by these thresholds, based on Monte Carlo transport calculations, correspond to higher energies that depend on the energy spectrum of the incident electrons. The E2, P2, P3, He, and HV measurements use coincidence detections between the two solid-state detectors.
- L. J. Lanzerotti *et al.*, *Science* **272**, 858 (1996).
- The HV channel may be dominated in some regions by interactions of energetic He with the telescope structure. We determined the fluxes using nominal geometrical factors and efficiencies. The geometrical factors used are 0.18 and 0.246 cm² sr for (E1 and P1) and (E2, P2, P3, He, and HV), respectively.
- K. R. Pyle, R. B. McKibben, J. A. Simpson, *J. Geophys. Res.* **88**, 45 (1983); R. B. McKibben, K. R. Pyle, J. A. Simpson, *ibid.*, p. 36.
- R. W. Fillius, C. E. Mcllwain, A. Mogro-Campero, *Science* **188**, 465 (1975).
- J. H. Trainor, F. B. McDonald, D. E. Stilwell, B. J. Teegarden, W. R. Webber, *ibid.*, p. 462.
- J. A. Van Allen *et al.*, *ibid.*, p. 465.
- F. B. McDonald and J. H. Trainor, in *Jupiter*, T. Gehrels, Ed. (Univ. of Arizona Press, Tucson, AZ, 1976), p. 961.
- J. A. Simpson and R. B. McKibben, *ibid.*, p. 738.
- D. C. Jewitt and E. Danielson, *J. Geophys. Res.* **86**, 8691 (1981).
- I. dePater and C. K. Goertz, *ibid.* **95**, 39 (1990).
- E. Pehlke, thesis, Institut für Kernphysik, Universität Kiel, Germany (1988).
- We thank the NASA Ames Galileo Project Office, B. Chin, A. Wilhelm, C. Sobek, M. Smith, R. Young, and the technical staff for assistance during the long interval of excellent cooperation. We are grateful to F. Gliem and J. Bach (University of Braunschweig); F. Wendler, P. Glasow, and G. Eberlein (Siemens Company, Erlangen, Germany); the technical staff of the Dornier-System Company (Friedrichshafen, Germany); and the technical and administrative staff of VARTA Battery Company (Kelkheim and Hannover, Germany) for their help in making the LRD-EPI instrument a success. Thanks are due to E. Böhm (University of Kiel) for his contributions in scientific discussions and his assistance in data evaluation and with programs for particle track simulations in the detector telescope; S. Sievers (University of Kiel) for his help with the figures; and J. A. Van Allen (University of Iowa) for helpful suggestions. The EPI investigations were supported by the German Agency for Space Activities DARA by grant number 50 QJ 9001 7.

11 March 1996; accepted 22 April 1996

Radio Frequency Signals in Jupiter's Atmosphere

L. J. Lanzerotti, K. Rinnert, G. Dehmel, F. O. Gliem, E. P. Krider, M. A. Uman, J. Bach*

During the Galileo probe's descent through Jupiter's atmosphere, under the ionosphere, the lightning and radio emission detector measured radio frequency signals at levels significantly above the probe's electromagnetic noise. The signal strengths at 3 and 15 kilohertz were relatively large at the beginning of the descent, decreased with depth to a pressure level of about 5 bars, and then increased slowly until the end of the mission. The 15-kilohertz signals show arrival direction anisotropies. Measurements of radio frequency wave forms show that the probe passed through an atmospheric region that did not support lightning within at least 100 kilometers and more likely a few thousand kilometers of the descent trajectory. The apparent opacity of the jovian atmosphere increases sharply at pressures greater than about 4 bars.

Electrical discharges in Earth's atmosphere have long been of interest to humans as cultural, scientific, and technical phenomena (1). Electrical discharges in the atmospheres of other planets (2) are important for understanding atmospheric dynamics and may be significant in producing non-equilibrium chemical processes in a planetary atmosphere (3). For Jupiter, it has been shown theoretically that the nonthermal radio emissions (which are easily detectable from Earth) are not caused by lightning (4).

Optical evidence of lightning in the nightside jovian atmosphere found by the Voyager imaging systems (5) and the measurement of whistler-mode waves in the

jovian magnetosphere (6) suggested that electrical signals might be found by the Galileo probe. The lightning and radio emission detector (LRD) was designed (7) to be as flexible in its measuring capabilities as the probe on-board resources would allow. Many of the design decisions invoked knowledge of Earth lightning and extended the parameter limits by several factors of 10 in both directions. Because Jupiter has no well-defined surface close to the cloud system, it was believed that there would be no cloud-to-ground discharges, which are the best understood type of lightning on Earth. Cloud discharges on Earth are complex physical phenomena that generate a variety of radio frequency (RF) pulses and pulse trains (1).

Substantial efforts were made during probe development to reduce the electromagnetic interference (EMI) in the LRD from the subsystems in the probe. The LRD was tested during two flybys of Earth by Galileo in order to characterize the EMI noise expected during atmospheric entry. The acquired data demonstrated that only the net flux radiometer (NFR) (8) produced

L. J. Lanzerotti, Bell Laboratories, Lucent Technologies, Murray Hill, NJ 07974, and the University of Florida, Gainesville, FL 32611, USA.

K. Rinnert, Max-Planck-Institut für Aeronomy, D-37191 Katlenburg-Lindau, Germany.

G. Dehmel, F. O. Gliem, J. Bach, Universität Braunschweig, D-38106 Braunschweig, Germany.

E. P. Krider, University of Arizona, Tucson, AZ 85721, USA.

M. A. Uman, University of Florida, Gainesville, FL 32611, USA.

*Present address: Nortel Dasa Network Systems, D-88039 Friedrichshafen, Germany.